p-ISSN : 2335-1357 e-ISSN : 2437-1122

Mediterranean Journal of Modeling and Simulation

Med. J. Model. Simul. 10 (2018) 001-016

A Sliding Mode Observer Based Sensorless Vector Control of DFIG Based Wind Turbine

Noureddine Boumalha [a] *, Djillali Kouchih [b], Mohamed Seghir Boucherit [a]

[a] Process Control Laboratory, 10 Avenue H. Badi BP 182, Automatic control department, ENP Alger, Algeria

[b] Electronic Department, University Saad Dahlab, Blida, Algeria

ARTICLE INFO

Article history :
Received April 2018
Accepted August 2018

Keywords :
Wind Energy ;
DFIG ;
Vector Control ;
Sensorless ;
Sliding Mode Observer.

ABSTRACT

The modeling of a sliding mode observer which is used for the sensorless vector control of double fed induction generator (DFIG). The observer detects stator flux components in the phase stationary reference frame. The estimated rotor speed which is used in speed feedback loop is calculated by an adaptive observer based. The observer is adapted using a simple algorithm. Stability analysis based on Lyapunov theory is performed in order to guarantee the closed loop stability. Simulation tests under load disturbance are provided to evaluate the consistency and performance of the proposed control technique in the low and high speeds.

1. Introduction

Wind generation is one type of renewable energy resource that has been the focus of renewable energy profile in states with strong wind resources [17, 22].Practically, the doubly fed induction generators (DFIG). Sensorless vector control systems for Doubly Fed Induction Generators (DFIG) baeed wind turbine. Have been previously published by several researchers. Most of the earlier work is based on open loop methods, where the estimated and measured rotor currents are compared in order to derive the rotor position. The estimation of the rotor flux and speed is based on an adaptive observer. The controlled quantities are calculated using stability analysis based on Lyapunov theory. For controlled of DFIG, the parametric variation modifies the performances of the control system when we use a control law with fixed parameters [3, 25]. However, the performances will be degraded to high speed of wind turbine. To offer control robustness, the Variable Structure Control possesses this robustness. This problem can be remedied by replacing the switching function by a smooth continuous function [6]. The sensorless control method

*Email : boumalhanoureddine@yahoo.fr

is implemented by Matlab/simulink and several steady results are given and confirm the validity of the approach.

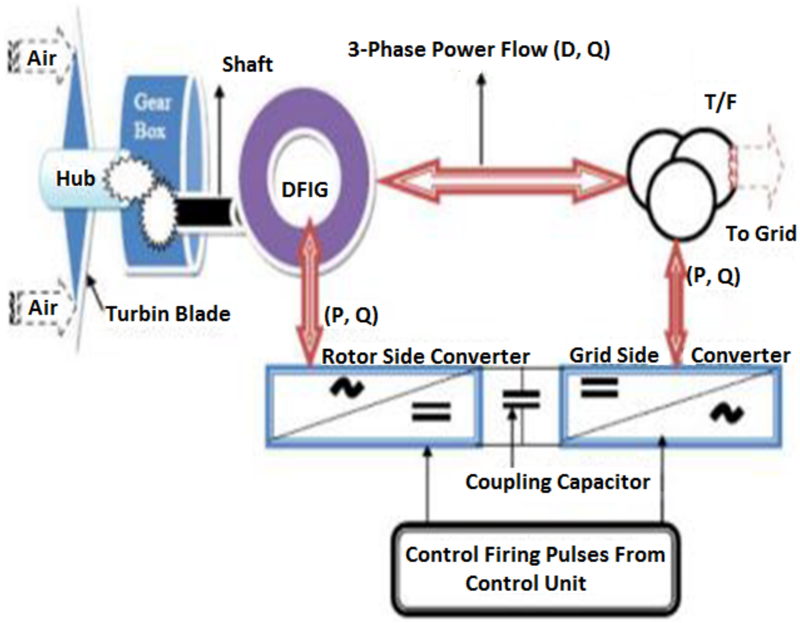

Fig. 1 – Configuration of a DFIG wind turbine system

2. System Modelling

2.1. Model in a-b-c coordinate reference frame

The DFIG can be modelled as following where the voltage equations of stator and rotor can be expressed using matrix notation by [10, 18] :

$$[V_s] = [R_s]\,[I_s] + \frac{d\,[\psi_s]}{dt} \tag{1}$$

$$[V_r] = [R_r]\,[I_r] + \frac{d\,[\psi_r]}{dt} \tag{2}$$

Where : the vector of voltages, currents and flux of stator and rotor windings are respectely.

$$[V_s] = [V_{sa}\ V_{sb}\ \ V_{sc}]^t,\ [V_r] = [V_{ra}\ V_{rb}\ \ V_{rc}]^t$$

$$[I_s] = [I_{sa}\ I_{sb}\ \ I_{sc}]^t,\ [I_r] = [I_{ra}\ I_{rb}\ \ I_{rc}]^t$$

$$[\psi_s] = [\psi_{sa}\ \psi_{sb}\ \ \psi_{sc}]^t,\ [\psi_r] = [\psi_{ra}\ \psi_{rb}\ \ \psi_{rc}]^t$$

The stator and rotor resistances matrices are given by

$$[R_s] = \begin{bmatrix} R_s & 0 & 0 \\ 0 & R_s & 0 \\ 0 & 0 & R_s \end{bmatrix}, \; [R_r] = \begin{bmatrix} R_r & 0 & 0 \\ 0 & R_r & 0 \\ 0 & 0 & R_r \end{bmatrix}$$

Where : R_s and R_r resistance of stator and rotor windings. The instantaneous stator and rotor flux per phase are given by :

$$[\psi_s] = [L_{ss}] [I_s] + [M_{sr}] [I_r] \tag{3}$$

$$[\psi_r] = [L_{rr}] [I_r] + [M_{rs}] [I_s] \tag{4}$$

Where :

$$[L_{ss}] = \begin{bmatrix} L_{aa} & L_{ab} & L_{ac} \\ L_{ba} & L_{bb} & L_{bc} \\ L_{ca} & L_{cb} & L_{cc} \end{bmatrix}, \; [L_{rr}] = \begin{bmatrix} L_{AA} & L_{AB} & LAC \\ L_{BA} & L_{BB} & L_{BC} \\ L_{CA} & L_{CB} & L_{CC} \end{bmatrix} \tag{5}$$

The mutual inductances matrix can be written :

$$[M_{sr}] = M_s \begin{bmatrix} \cos(\theta_r) & \cos\left(\theta_r + \frac{2\pi}{3}\right) & \cos\left(\theta_r - \frac{2\pi}{3}\right) \\ \cos\left(\theta_r - \frac{2\pi}{3}\right) & \cos(\theta_r) & \cos\left(\theta_r + \frac{2\pi}{3}\right) \\ \cos\left(\theta_r + \frac{2\pi}{3}\right) & \cos\left(\theta_r - \frac{2\pi}{3}\right) & \cos(\theta_r) \end{bmatrix} \tag{6}$$

Where :
M_{sr} : stator/rotor mutual inductances
L_r ,L_s : rotor and stator winding inductances.
Replace the relations (3) and (4) respectively in equations (1) and (2) ; we obtain the following two expressions : [1, 2, 9]

$$\begin{cases} V_s = [R_s] [I_s] + [L_{ss}] \frac{d}{dt} [I_s] + \frac{d}{dt} [M_{sr}] [I_r] \\ V_r = [R_r] [I_s] + [L_{rr}] \frac{d}{dt} [I_r] + \frac{d}{dt} [M_{sr}]^t [I_s] \end{cases} \tag{7}$$

The electromagnetic torque is given by the following general expression [11, 12] :

$$C_{em} = p [I_s] \frac{d [M_{sr}] [I_r]}{dt}$$

2.2. Modeling of DFIG with rotor short-circuit fault modeling

The modelling of DFIG rotor inter-turn short-circuit fault is similar to the previous case following the same steps.

The new form of rotor voltages equations are rewritten as follows : [11, 12]

$$[V_r] = [R_r] [I_r] + \frac{d [\psi_r]}{dt} \tag{8}$$

Where :

$[V_r] = [V_{ra}\ V_{rb}\ \ V_{rc}\ \ V_{rd}]^t$, $[I_r] = [I_{ra}\ I_{rb}\ \ I_{rc}\, I_{rd}]^t$

$[\psi_r] = [\psi_{ra}\ \psi_{rb}\ \ \psi_{rc}\ \psi_{rd}]^t$

The rotor resistance matrix can be rewritten as follows : [7, 19]

$$[R_r] = \begin{bmatrix} (1-\gamma)\,R_r & 0 & 0 & \gamma.R_r \\ 0 & R_r & 0 & 0 \\ 0 & 0 & R_r & 0 \\ 0 & 0 & 0 & \gamma.R_r \end{bmatrix} \tag{9}$$

We will have the new inductance rotorique matrix following :

$$[L_{rr}] = L_{frs}\,diag\left[(1-\gamma)\ \ 1\ 1\ \gamma\right] + M_r \begin{bmatrix} (1-\gamma)^2 & -\frac{(1-\gamma)}{2} & -\frac{(1-\gamma)}{2} & \gamma\,(1-\gamma) \\ -\frac{(1-\gamma)}{2} & 1 & -\frac{1}{2} & -\frac{\gamma}{2} \\ -\frac{(1-\gamma)}{2} & -\frac{1}{2} & 1 & -\frac{\gamma}{2} \\ \gamma\,(1-\gamma) & -\frac{\gamma}{2} & -\frac{\gamma}{2} & \gamma^2 \end{bmatrix} \tag{10}$$

And the matrix of mutual inductances is : [4, 20]

$$[M_{sr}] = M_s \begin{bmatrix} (1-\gamma)\cos(\theta_r) & (1-\gamma)\cos\left(\theta_r - \frac{2\pi}{3}\right) & (1-\gamma)\cos\left(\theta_r + \frac{2\pi}{3}\right) \\ \cos\left(\theta_r + \frac{2\pi}{3}\right) & \cos(\theta_r) & \cos\left(\theta_r - \frac{2\pi}{3}\right) \\ \cos\left(\theta_r - \frac{2\pi}{3}\right) & \cos\left(\theta_r + \frac{2\pi}{3}\right) & \cos(\theta_r) \\ \gamma\cos(\theta_r) & \gamma\cos\left(\theta_r - \frac{2\pi}{3}\right) & \gamma\cos\left(\theta_r + \frac{2\pi}{3}\right) \end{bmatrix} \tag{11}$$

3. Vector Control of DFIG

In order to establish a vector control of DFIG, we recall here its modelling in the Park frame. The equations of the stator voltages and rotor of the DFIG are defined by : (1) and (2)

$$\begin{cases} V_{ds} = R_s.i_{ds} + \frac{d}{dt}\left[\psi_{ds}\right] - \omega_s\psi_{qs} \\ V_{qs} = R_s.i_{qs} + \frac{d}{dt}\left[\psi_{qs}\right] + \omega_s\psi_{ds} \\ V_{dr} = R_r.i_{dr} + \frac{d}{dt}\left[\psi_{dr}\right] - \omega_r\psi_{qr} \\ V_{qr} = R_r.i_{qr} + \frac{d}{dt}\left[\psi_{qr}\right] + \omega_r\psi_{dr} \end{cases} \tag{12}$$

The equations of stator and rotor flux are given as follows : [21, 23]

$$\begin{cases} \psi_{ds} = L_s.i_{ds} + M_{sr}.i_{dr} \\ \psi_{qs} = L_s.i_{qs} + M_{sr}.i_{qr} \\ \psi_{dr} = L_r.i_{dr} + M_{rs}.i_{ds} \\ \psi_{qr} = L_r.i_{qr} + M_{rs}.i_{qs} \end{cases} \tag{13}$$

The electromagnetic torque can be expressed by : [16, 15]

$$C_{em} = p\frac{M_{sr}}{L_r}\left(\psi_{ds}I_{qr} - \psi_{qs}I_{dr}\right) \tag{14}$$

We obtain Tthe rotor voltages as a function of rotor currents as follows :

$$\begin{cases} V_{dr} = \left[R_r + \left(L_r - \frac{M_{sr}^2}{L_s}\right) S\right] I_{dr} - g\omega_s \left(L_r - \frac{M_{sr}^2}{L_s}\right) I_{qr} \\ V_{qr} = \left[R_r + \left(L_r - \frac{M_{sr}^2}{L_s}\right) S\right] I_{qr} + g\omega_s \left(L_r - \frac{M_{sr}^2}{L_s}\right) I_{dr} + g\omega_s \frac{M_{sr}V_s}{\omega_s L_s} \end{cases} \tag{15}$$

The generator is connected directly to the power network side of the stator over the rotor circuit the power network from the stator side, the rotor circuit is powered by a DC source assumed constant through an inverter controlled by the PWM technique (Fig.2). gives. We will adopt conventional controllers (PI) necessary to achieve control of reactive power and adjusting the speed of the DFIG. The control of rotor currents is done by regulators Proportional Integral (PI) controllers. A PI controller is also used for adjusting reactive power controller, as shown in the figure (2). [13, 14].

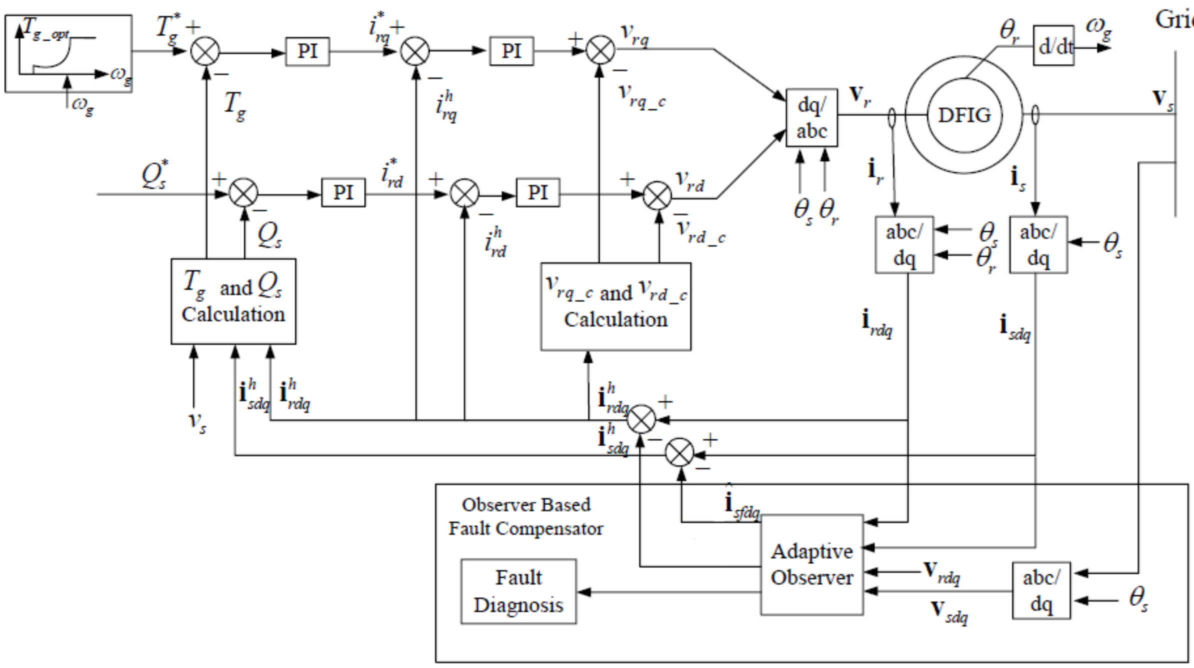

Fig. 2 – Block diagram of speed and reactive power controls of DFIG

4. DFIG in State Space

From equations (1) and (2), the dynamic model developed of the DFIG under the stationary $(\alpha\beta)$ reference is obtained as follows :

$$\begin{cases} \frac{di\alpha s}{dt} = -\frac{1}{\sigma Ls}\left(R_s + R_r\frac{L_m^2}{L_r^2}\right) i\alpha s + \frac{1}{\sigma Ls} R_r \frac{Lm}{L_r^2}\Phi_{\alpha r} + \frac{1}{\sigma Ls}\omega\frac{Lm}{L_r}\Phi_{\beta r} + \frac{1}{\sigma Ls} v\alpha s + \frac{L_m}{\sigma Ls L_r} v\alpha r \\ \frac{di\beta s}{dt} = -\frac{1}{\sigma Ls}\left(R_s + R_r\frac{L_m^2}{L_r^2}\right) i\beta s - \frac{1}{\sigma Ls}\omega\frac{Lm}{L_r}\Phi_{\alpha r} + \frac{1}{\sigma Ls} R_r \frac{Lm}{L_r^2}\Phi_{\beta r} + \frac{1}{\sigma Ls} v\beta s + \frac{L_m}{\sigma Ls L_r} v\beta r \\ \frac{d\Phi\alpha r}{dt} = \frac{RrLm}{Lr} i\alpha s - \frac{Rr}{Lr}\Phi\alpha r - \omega\Phi\beta r + v\alpha r \\ \frac{d\Phi\beta r}{dt} = \frac{RrLm}{Lr} i\beta s - \frac{Rr}{Lr}\Phi\beta r + \omega\Phi\alpha r + v\beta r \end{cases}$$

The model of the observer is written frame. [5, 7, 8]

$$\left\{ \begin{array}{l} \frac{d\hat{X}}{dt} = \hat{A}\hat{X} + BU + G\left(Y - \hat{Y}\right) \\ \hat{Y} = C\hat{X} \end{array} \right. \tag{16}$$

With

$$X = [i_{\alpha s}\ i_{\beta s}\ \ \Phi_{\alpha r}\ \ \Phi_{\beta r}]^{\,t}, Y = \begin{pmatrix} i\alpha s \\ i\beta s \end{pmatrix}$$

$$u = [u_{\alpha s}\ u_{\beta s}\ \ u_{\alpha r}\ \ u_{\beta r}]^{\,t}$$

$$A = \begin{bmatrix} A_{11} & A_{12} \\ A_{21} & A_{22} \end{bmatrix}$$

$$B = \begin{bmatrix} B_{11} & B_{12} \\ B_{21} & B_{22} \end{bmatrix}$$

$$I = \begin{bmatrix} 1 & 0 \\ 0 & 1 \end{bmatrix}$$

$$J = \begin{bmatrix} 0 & -1 \\ 1 & 0 \end{bmatrix}$$

With

$$A_{11} = \begin{bmatrix} \left(\frac{-1}{\sigma\,\tau_s} - \frac{L_m^2}{\tau_s \sigma L_s\,L_r}\right) & 0 \\ 0 & \left(\frac{-1}{\sigma\,\tau_s} - \frac{L_m^2}{\tau_s \sigma L_s\,L_r}\right) \end{bmatrix}$$

$$A_{12} = \begin{bmatrix} \frac{L_m}{\tau_r \sigma L_s\,L_r} & \frac{wL_m}{\sigma L_s\,L_r} \\ \frac{wL_m}{\sigma L_s\,L_r} & \frac{L_m}{\tau_r \sigma L_s\,L_r} \end{bmatrix}$$

$$A_{21} = \begin{bmatrix} \frac{L_m}{\tau_r} & 0 \\ 0 & \frac{L_m}{\tau_r} \end{bmatrix}$$

$$A_{22} = \begin{bmatrix} \frac{-1}{\tau_r} & -w \\ w & \frac{-1}{\tau_r} \end{bmatrix}$$

$$B_{11} = \begin{bmatrix} \frac{1}{\sigma\,L_s} & 0 \\ 0 & \frac{1}{\sigma\,L_s} \end{bmatrix}$$

$$B_{12} = \begin{bmatrix} \frac{-L_m}{\sigma L_s\,L_r} & 0 \\ 0 & \frac{-L_m}{\sigma L_s\,L_r} \end{bmatrix}$$

$$B_{21} = \begin{bmatrix} 0 & 0 \\ 0 & 0 \end{bmatrix}$$

$$B_{22} = \begin{bmatrix} 1 & 1 \\ 1 & 1 \end{bmatrix}$$

$$\tau_r = \frac{L_r}{R_r}$$

We define

$$\delta\omega = \omega - \hat{\omega} \tag{17}$$

The symbol $\wedge$ denotes estimated values and G is the observer gain matrix. We will determine the differential system describing the evolution of the error

$$e = X - \hat{X} \tag{18}$$

The state matrix of the observer can be written as

$$\hat{A} = A + \delta A \tag{19}$$

With

$$\delta A = \begin{pmatrix} 0 & 0 & 0 & +\frac{Lm}{b}\delta\omega \\ 0 & 0 & -\frac{Lm}{b}\delta\omega & 0 \\ 0 & 0 & 0 & -\delta\omega \\ 0 & 0 & +\delta\omega & 0 \end{pmatrix} \tag{20}$$

Then, we can write

$$\frac{d\hat{X}}{dt} = \hat{A}\hat{X} + BU + G\left(Y - \hat{Y}\right)$$

$$\frac{de}{dt} = (A - GC)\,e - \delta A\hat{X}$$

We define the Lyapunov function

$$V = e^T e + \frac{(\delta\omega)^2}{\lambda} \tag{21}$$

λ is a positive scalar.

This function should contain terms of the difference and to obtain mechanism adaptation. The stability of the observer is guaranteed for the condition

$$\frac{dV}{dt} < 0$$

We obtain the adaptation mechanism in the form

$$\hat{\omega} = \int_0^t \lambda \ \left[\frac{L_m}{b} \left(\hat{\Phi}_{\beta s} \, e_{i\alpha s} - \hat{\Phi}_{\alpha r} \, e_{i\beta s} \right) \right] dtt \tag{22}$$

The matrix of gain G is selected such as the eigenvalues of the matrix A-GC .
The estimated electromagnetic torque is expressed

$$\hat{C}_e = \frac{3}{2} p \frac{L_m}{L_r} \left(\hat{\Phi}_{\alpha r} \hat{\imath}_{\beta s} - \hat{\Phi}_{\beta r} \hat{\imath}_{\alpha s} \right) \tag{23}$$

5. Sliding Mode Observer

5.1. Principle of a sliding-mode observer

We consider nonlinear system of the form : [19, 26]

$$\begin{cases} \dot{x}(t) = f(x(t), u(t)) \\ y(t) = Cx(t) \end{cases} \tag{24}$$

where

$x \in R^n, u \in R^m$

$y \in R^p$

We assume that the system is observable, for the system (28), we define the observer by sliding mode by : [24]

$$\dot{\hat{x}} = f(\hat{x}(t), u(t)) + \Lambda I_s \tag{25}$$

Or $\hat{x} \in R^n$, $\Lambda \in R^{n*p}$ is the matrix of the observation gains to be specified and is the vector of discontinuous sign :

$$I_s = Sign\,(S) = [sign\,(s_1)\,, sign\,(s_2)\,.....sign\,(s_p)\,,]^{\mathrm{T}} \tag{26}$$

Where is the classic sign function and is the next slip surface

$$S = NC\overline{x} = [s_1,\ s_2......s_p] \tag{27}$$

$$\bar{x} = x - \hat{x} \tag{28}$$

Or $N \in R^{PxP}$ is a matrix to be specified
Thus, the dynamics of the observation error becomes :

$$\dot{\hat{x}} = f(x, u) - \hat{f}(\hat{x}, u) + \Lambda I_s \tag{29}$$

5.2. Sliding mode observer applied to the DFIG

The sliding mode observer proposed for the estimation of the DFIG flows :

$$\begin{cases} \dot{\hat{x}}_1 = ax_1 + \frac{R_r L_m}{aL_r}\hat{x}_3 + \frac{L_m}{b}\hat{x}_4 p x_5 + \frac{1}{\sigma L_s}\nu_{\alpha r} + \Lambda_1^T I_s \\ \dot{\hat{x}}_2 = ax_2 - \frac{L_m}{b}\hat{x}_3 p x_5 + \frac{R_r L_m}{aL_r}\hat{x}_4 + \frac{1}{\sigma L_s}\nu_{\beta s} + \Lambda_2^T I_s \\ \dot{\hat{x}}_3 = \frac{R_r L_m}{L_r}x_1 - \frac{R_r}{L_r}\hat{x}_3 - \hat{x}_4 p x_5 + \nu_{ar} + \Lambda_3^T I_s \\ \dot{\hat{x}}_4 = \frac{R_r L_m}{L_r}x_2 - \frac{R_r}{L_r}\hat{x}_4 - \hat{x}_3 p x_5 + \nu_{\beta r} + \Lambda_4^T I_s \\ \dot{\hat{x}}_5 = d\left(\hat{x}_3 x_2 - \hat{x}_4 \hat{x}_1\right) - \frac{T_r}{J} - \frac{f_v}{J}x_5 = q_1\left(x_5 - \hat{x}_5\right) + \Lambda_5^T I_s \end{cases} \tag{30}$$

$$a = \frac{1}{\sigma L_s}\left(R_s + R_r \frac{L_m^2}{L_r^2}\right)$$

$$b = \sigma L_s L_r$$

$$\sigma = 1 - \frac{L_m^2}{L_s L_r}$$

With

$$\hat{x} = \begin{bmatrix} \hat{\imath}_{\alpha s} & \hat{\imath}_{\beta s} & \hat{\Phi}_{\alpha r} & \hat{\Phi}_{\beta r} & \hat{w}_r \end{bmatrix}$$

$$\hat{y} = \begin{bmatrix} \hat{\imath}_{\alpha s} & \hat{\imath}_{\beta s} & \hat{w}_r \end{bmatrix}$$

$$I_s = \begin{bmatrix} sign\left(S_1\right) & sign\left(S_2\right) \end{bmatrix}^T$$

$$\begin{cases} S_1 = x_1 - \hat{x}_1 \\ S_2 = x_2 - \hat{x}_2 \end{cases}$$

S_1 and S_2 represent the sliding surfaces.

The gains : q_1, Λ_1^T, Λ_2^T, Λ_3^T, Λ_4^T, Λ_5^T are calculated to ensure the asymptotic convergence of the error estimate. They are given by :

$$\begin{array}{l} \begin{bmatrix} \Lambda_1^T \\ \Lambda_2^T \end{bmatrix} = D^{-1}\begin{bmatrix} \delta_1 & 0 \\ 0 & \delta_2 \end{bmatrix} \text{ and } D = \frac{1}{\left(\alpha^2 + (kpx_5)^2\right)}\begin{bmatrix} \alpha & -kpx_5 \\ kpx_5 & \alpha \end{bmatrix} \\ \begin{bmatrix} \Lambda_{31} & \Lambda_{32} \\ \Lambda_{41} & \Lambda_{42} \end{bmatrix} = \left[\begin{pmatrix} -c & -px_5 \\ px_5 & -c \end{pmatrix}\begin{pmatrix} q_3 & 0 \\ 0 & q_4 \end{pmatrix}\right]\begin{pmatrix} \delta_1 & 0 \\ 0 & \delta_2 \end{pmatrix} \\ \begin{bmatrix} \frac{\Lambda_{51}}{\delta_1} & \frac{\Lambda_{52}}{\delta_2} \end{bmatrix} = d\begin{bmatrix} x_2 & -x_1 \end{bmatrix} \end{array} \tag{31}$$

Sach as :

$$\begin{cases} \delta_1 > |e_3|_{\max} \\ \delta_2 > |e_4|_{\max} \end{cases}$$

$$\begin{cases} q_1 > 0 \\ q_3 > 0 \\ q_4 > 0 \end{cases}$$

The residual signal is calculated as follows, $r = [y - \hat{y}]$ and we define as the detection threshold (lower limit).

6. Simulation Results

The technique presented has been implemented in the MATLAB /simulink. The simulation test involves the wind speed variation and the reactive power reference constant equals to zero, as shown in the table below :

Table 1 – Variation of wind speed

t (s)	0	4	7
V (m/s)	12	17	16
Q_{sref} (var)	0	0	0

6.1. The healthy operation

To illustrate the performance of the proposed sensorless control, we will study several modes of operation. The first mode corresponds to the over speed operation. Then we treat the healthy functioning. Finally, we will study the impact of the following disturbances : high speed.

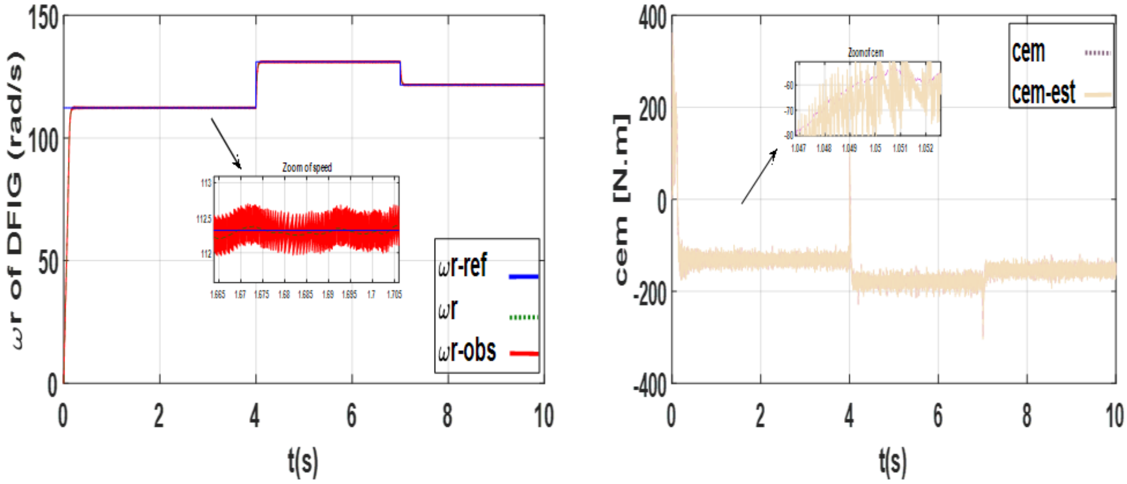

Fig. 3 – Rotation speed and electromagnetic torque of the DFIG

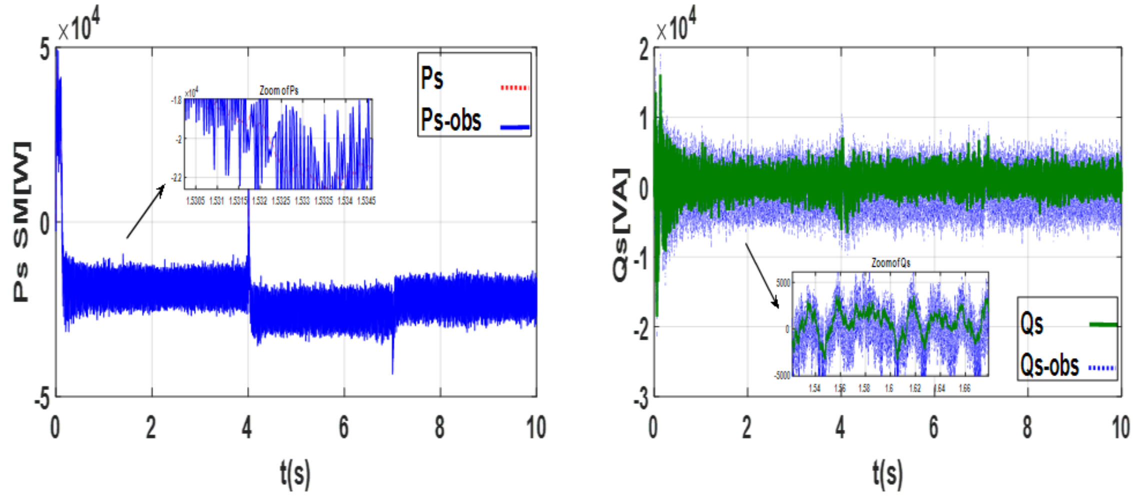

Fig. 4 – Active and reactive stator power with variation of wind speed

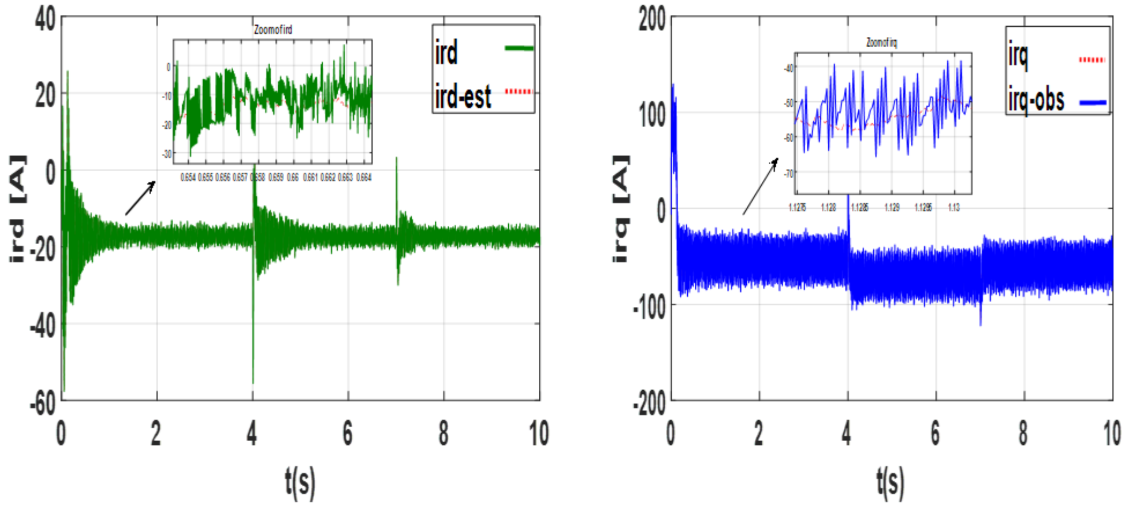

Fig. 5 – Park's rotor currents (i_{rd}, i_{rq}) with variation of wind speed

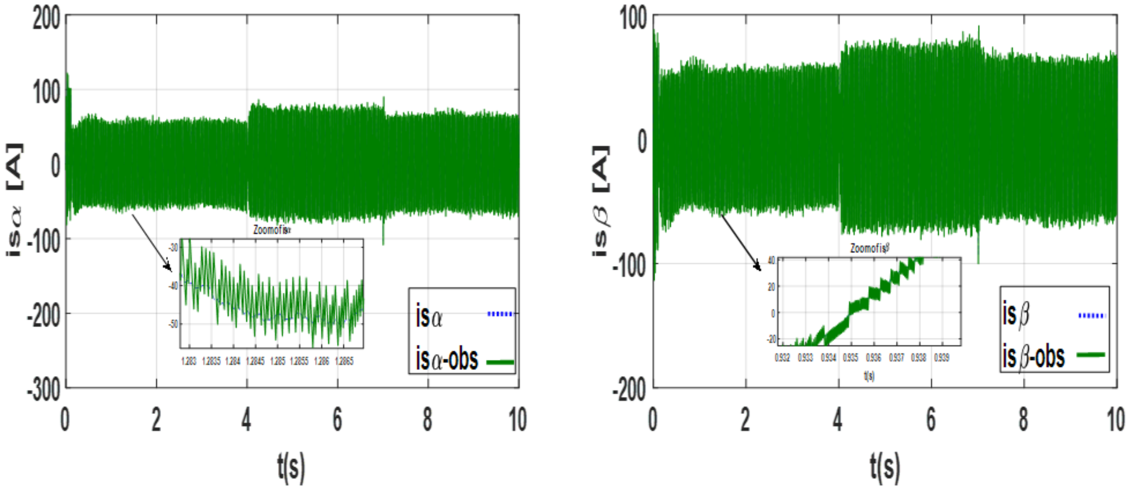

Fig. 6 – Stator currents $(I_{s\alpha}, I_{s\beta})$ with variation of wind speed

6.2. Operation with high speed

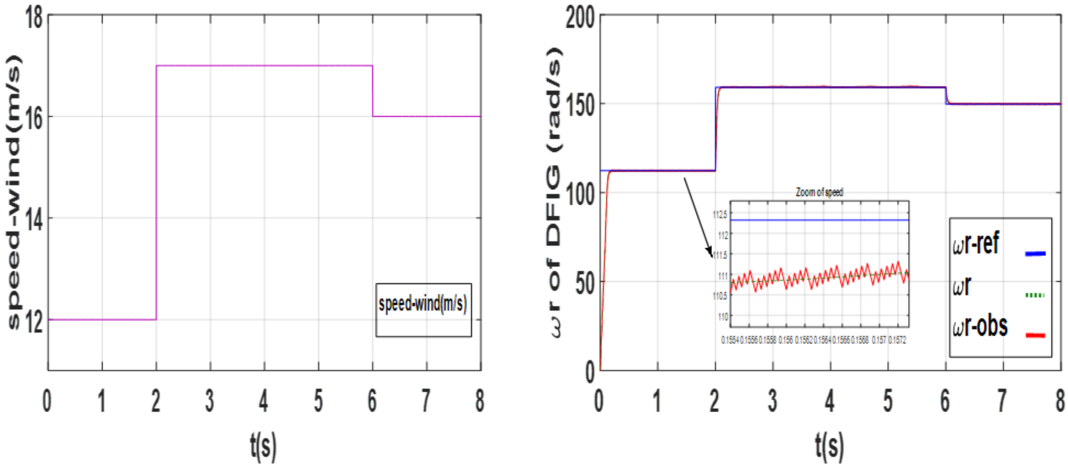

Fig. 7 – Variation of wind speed and rotation speed of the DFIG

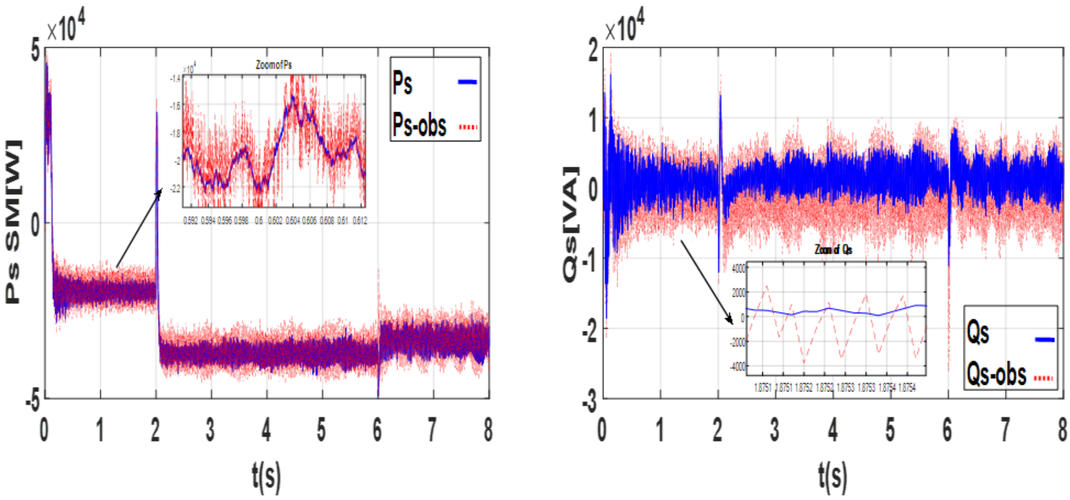

Fig. 8 – Active and reactive stator power

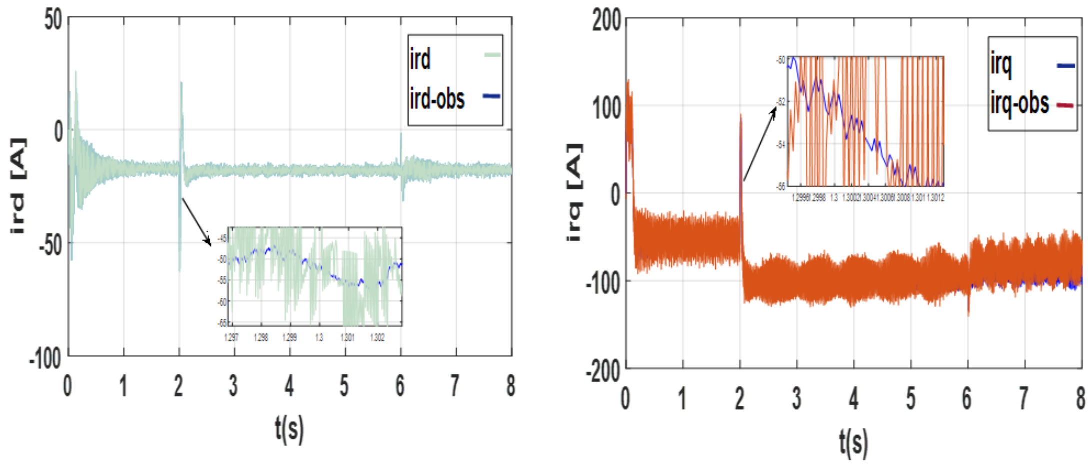

Fig. 9 – Park's rotor currents (i_{rd}, i_{rq})

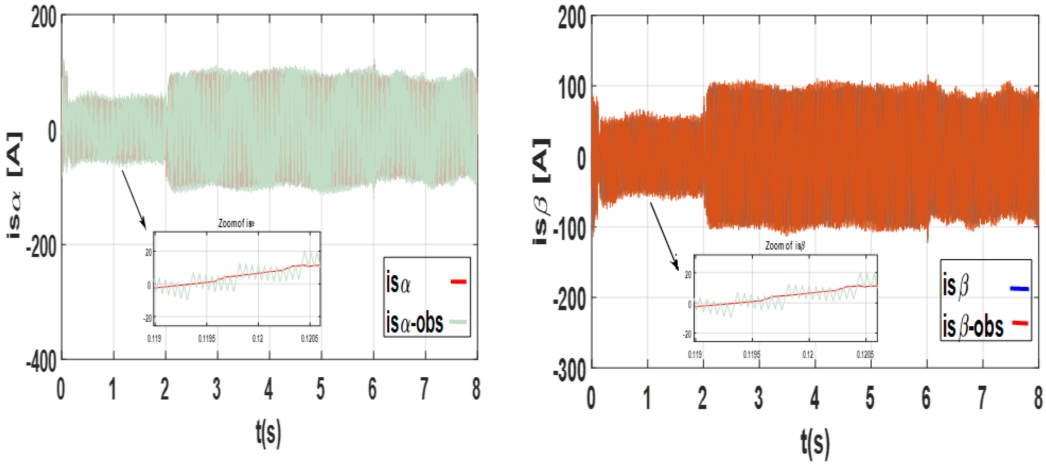

Fig. 10 – Stator Current $(I_{s\alpha}, I_{s\beta})$

6.3. Interpretation of results

The present rotational speed of the ripple relative to the healthy operation is noted. The active and reactive stator power and the direct and quadrature rotor currents and the stator phase current have oscillations of higher amplitudes than those corresponding to the healthy operation. Consequently, the control with sliding mode observer has good performances of robustness and precision of operation in degradation against high speed.

6.4. Spectral analysis in the DFIG

6.4.1. Introduction

In this section we will present the application of the technique of three-phase stator current spectral analysis, of the Park vector module for detection of the DFIG. The simulations are made for a supposedly constant wind speed equal to 12 m/s and the reference reactive power 0var. the calculation is performed under the MATLAB/Simulink environment with a calculation step of 0.03ms.

6.4.2. Spectral analysis of the current of the stator phase "a"

(Fig.11), We notice that the spectrum of the three-phase stator current appear harmonics (close to the fundamental) which corresponds to the supply frequency $fs = 50Hz$.

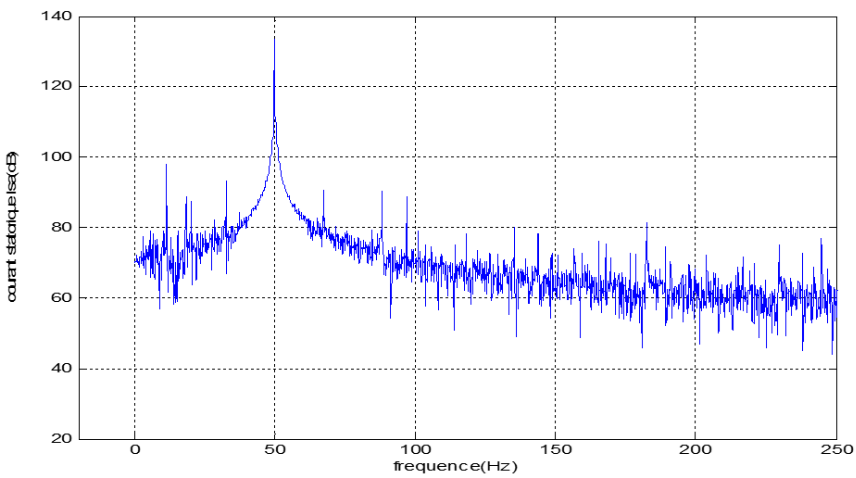

Fig. 11 – Three - phase stator current spectrum

7. Conclusion

A new approach to doubly-fed induction generator (DFIG) based wind turbine modeling has been presented. It can be readily applied for the analysis of healthy of the DFIG. The global control scheme introduces high performances of robustness ; stability and precision, particularly, under uncertainty caused by load variation. Furthermore, this observation method presents a simple algorithm that has the advantage to be easily implantable in a calculator. The sliding mode observer uses an adaptation mechanism for the rotor flux and speed estimation. This approach relies on the improvement of an estimation of the rotor flux components and rotor speed. The estimation of the rotor flux has well made more robust and more stable the DFIG based Vector Control. Through simulation strategy has been validated steady-state conditions by Matlab/simulink.

Acknowledgments

The authors deeply appreciate the support obtained from ENP (Automatic control department, ENP Alger, Algeria) and USDB (Electronic Department, University Saad Dahlab, Blida, Algeria) which has permitted the participation and presentation of this work .

REFERENCES

[1] Adam MIRECKI : Etude comparative de chaines de conversion d.energie dediees a une éolienne de petite puissance. These doctorat de l.Institut National Polytechnique de Toulouse, Avril 5, (2005).

[2] A. Ur Rehman, Yu Chen : Simulation using MATLAB/Simulink on Rotor Winding Inter-turn Short Circuit Fault in DFIG. Xi'an Jiaotong University Xi'an, Shaanxi, China, (2016).

[3] B. Chitti Babu, K.B. Mohanty : Doubly-Fed Induction Generator for Variable Speed Wind Energy Conversion Systems- Modeling & Simulation. International Journal of Computer and Electrical Engineering, Vol. 2, No. 1, February, (2010).

[4] C. Wei, Z. Zhang : Stator Current-Based Sliding Mode Observer for Sensorless Vector Contorl of Doubly-Fed Induction Geneartors. IEEE Trans. on Application 3, (2015) , 978-1-4673-7151.

[5] D. Casadei, A. Yazidi : Diagnostic Technique based on Rotor Modulating Signals Signature Analysis for Doubly Fed Induction Machines in Wind Generator Systems. IEEE Industry Applications Conference, (2006). 41st IAS Annual Meeting Conference Record , (2006), pp. 1525 – 1532.

[6] D. Kouchih, R. Hachelaf, N. Boumalha, M. Tadjine, and M.S. Boucherit : Vector fault tolerant control of induction motor drives subject to stator interturn faults. The 16th Power Electronics and Motion Control Conference and Exposition, Antalya, Turkey, September 21-24, (2014).

[7] D. Kouchih ; M. Tadjine ; and M.S. Boucherit : Analysis of controlled induction motor drives with stator faults, International Symposium on Environment Friendly energies and Applications, Northumbria university, Newcastle upon Tyne, United Kingdom, (2012).

[8] D. Kouchih ; M. Tadjine ; and M.S. Boucherit : Analysis of controlled induction motor drives with stator faults, International Symposium on Environment Friendly energies and Applications, Northumbria university, Newcastle upon Tyne, United Kingdom, (2012).

[9] D. Casadei, A. Yazidi : Diagnostic Technique based on Rotor Modulating Signals Signature Analysis for Doubly Fed Induction Machines in Wind Generator Systems. IEEE Industry Applications Conference, (2006). 41st IAS Annual Meeting Conference Record , (2006), pp. 1525 – 1532.

[10] F. Poitiers : Etude et Commande de Génératrices Asynchrones pour l'Utilisation de l'Energie Eolienne.Thèse de doctorat, Nantes, (2003).

[11] F. Poitiers, T. Bouaouiche, M. Machmoum : Advanced control of a doubly-fed induction generator for wind energy conversion. Electric Power Systems Research Volume 79, (2009). pp. 1085-1096.

[12] H. Camblong : Minimisation de l'Impact des Perturbations d'Origine Eolienne dans la Generation d.Electricite par des Aerogenerateurs a Vitesse Variable. These de Doctorat en Automatique, Ecole Nationale Superieure d.Arts et Metiers, Centre de Bordeaux, France, (2003).

[13] J. Zafar, J. Gyselinck : CUSUM based Fault Detection of Stator Winding Short Circuits in Doubly Fed Induction Generator based Wind Energy Conversion Systems. Department of Electrical Engineering Université Libre de Bruxelles (ULB) CP165/52, 50 Av. F.D. Roosevelt, 1050 Brussels, Belgium, (2010).

[14] Jawwad ZAFAR : Winding Short-Circuit Fault Modelling and Detection in Doubly-Fed Induction Generator based Wind Turbine Systems. Phd Thesis, Université libre de Bruxeles, Faculty of Applied Sciences Department of Electrical Engineering, October 13, (2011).

[15] Jesper S. Thomsen and Carsten S. Kallesϕe, Stator fault modeling of induction motors, IEEE Int. Symposium on Power Electronics, Eletrical Drives, Automation and Motion, pp.1275-1280, (2006).

[16] L. Holdsworth, X.G. Wu, J.B. Ekanayake, N. Jenkins : Comparison of fixed speed and doubly-fed induction wind turbines during power system disturbance. Proc. Gener. Transm. Distrib., 150(3), (2003). pp. 343-352.

[17] M.E.H. Benbouzid : Bibliography on induction motors fault detection and diagnosis. IEEE Trans. on Energy Conversion, 14 (4) , (1999). pp. 1065–1074.

[18] M. E. H. Benbouzid : Review of induction motors signature analysis as a medium for faults detection. IEEE Trans. on Industrial Electronics, 47 (5) , (2000). pp. 984–993.

[19] N. Benouzza, A. Benyettou, A. Bendiabdellah, B. Kraloua ,D. Toumi : Rotor Cage Faults Diagnosis in 3 Phase Induction Motors, by Park's Vector Approach. Jordanian International Electrical Electronics Engineering Conference, (2001).

[20] R. M.Tallam, T. G. Habetler, R.G. Harley : Transient model for induction machines with stator winding turn faults.IEEE Trans. on Application, 38(3) , (2002). pp. 632-637.

[21] S. Ebrahimkhani : Robust fractional order sliding mode control of doubly-fed induction generator -based wind turbines . ISA Transactions , (2016).

[22] S. Shao, E. Abdi, F. Barati, R. McMahon : Stator-Flux-Oriented Vector Control for Brushless Doubly Fed Induction Generator. IEEE Transactions. On Industrial

Electronics, Vol. 56, No. 10, (2009).

[23] T. Ghennam, E.M. Berkouk, B.François : Modeling and control of a doubly fed induction generator (DFIG) based wind conversion system. International Conference on Power Engineering, Energy and Electrical Drives, (2009). POWERENG

[24] X. Zheng, R. Song : Full-order terminal sliding mode stator flux observer for DFIG. IEEE Trans. on Application, (2016) , 978-1-4673-8644-9.

[25] X. Cheng, V. Cocquempot and C. Christophe, A model of asynchronous machine for stator fault detection and isolation, IEEE Trans. Ind. Eletron., vol. 50, no. 3, pp. 578-584, (2003).

[26] Y. Gritli, A. Stefani, F. Filippetti and A. Chatti, Stator fault analysis based on wavelet technique for wind turbines equipped with DFIG, In Proceeding of IEEE International Conference on Clean Electrical Power, Capri, Italy, (2009), pp. 485-491.

Appendix 1 - Wind Turbine Parameters

Rated power : $P_s = 7500W$
Moment of the inertia : $J = 0.31125kg.m^2$
Wind turbine radius : $R = 3m$
Gear box ratio : $G = 5.4$
Air density : $\rho = 1.25kg/m^3$

Appendix 2 - DFIG Parameters

Rated power : $7500W$
Mutual inductance : $L_m = 0.0078H$
Stator leakage inductance : $L_s = 0.0083H$
Rotor leakage inductance : $L_r = 0.0081H$
Stator resistance : $R_s = 0.455\Omega$
Rotor resistance : $R_r = 0.62\Omega$
Number of pole pairs : $P = 2$
Moment of the inertia : $J = 0.31125kg.m^2$
Viscous friction : $fv = 0.00673kg.m^2.s^{-1}$